Journal of Membrane Science 466 (2014) 114–122

Contents lists available at ScienceDirect

Journal of Membrane Science

journal homepage: www.elsevier.com/locate/memsci

Wettability, pore structure and performance of perfluorodecyl-modified silica membranes

Qi Wei, Yuan-Li Ding, Zuo-Ren Nie*, Xiang-Ge Liu, Qun-Yan Li

College of Materials Science and Engineering, Beijing University of Technology, 100 Pingleyuan, Chaoyang District, Beijing 100124, PR China

ARTICLE INFO

Article history:
Received 10 January 2014
Received in revised form
28 March 2014
Accepted 19 April 2014
Available online 26 April 2014

Keywords:
Silica membrane
Perfluorodecyl groups
Wettability
Pore structure
Hydrothermal stability

ABSTRACT

Perfluorodecyl-modified silica membranes were prepared by the sol–gel technique using tetraethyl orthosilicate (TEOS) and 1H,1H,2H,2H-Perflouorodecyltriethoxysilane (PFDTES) as precursors under acidic and clean room conditions. The wettability and pore structure of the modified silica membranes were characterized by means of water contact angle measurement, Fourier translation infrared spectroscopy (FT-IR), solid state ^{29}Si magic angle spinning nuclear magnetic resonance (^{29}Si MAS NMR) and nitrogen adsorption. The membrane performances including gas permeation/separation and long-term hydrothermal stability were also investigated in detail. The results show that perfluorodecyl groups have been successfully incorporated, resulting in a transformation from hydrophility to hydrophobicity for the modified silica membranes. With a low PFDTES/TEOS molar ratio of 0.2, the modified silica membranes exhibit a water contact angle of $112.6 \pm 0.5^{\circ}$ and a pore size ranging from 0.45 to 0.9 nm. The hydrogen permeance increases with increasing temperatures, leading to a considerably high value of 9.71×10^{-7} mol m^{-2} s^{-1} Pa^{-1} at 300 °C. At such a temperature, the H_2/CO_2 permselectivity and binary gas separation factor are 7.19 and 12.11, respectively. Under a humid condition with a temperature of 250 °C and a water vapor molar ratio of 5%, the single H_2 permeance and H_2/CO_2 permselectivity remain almost constant for at least 200 h, indicating that the modified membranes possess an outstanding hydrothermal stability.

1. Introduction

Membranes play a key role in various energy industries involved in gas separation such as coal gasification [1–3], methane steam reforming [4,5] or partial oxidation [6,7], pervaporation [8,9] and so on because the removal of a certain product, for instance, hydrogen, from the resultant mixtures by a gas permeable and selective membrane is expected to accelerate the reaction process. Silica membranes, especially those derived from the sol–gel technique, are considered as promising candidates for gas separation due to their high thermal stability, high porosity and easily tunable pore size in the level of gas molecules. In recent years, a large amount of literature has focused on the application of silica membranes in gas separation, pervaporation and membrane reactors [10–16].

A large gas flux and selectivity, together with a long-term stability under harsh operating conditions, are necessarily required for membrane applications in the above-mentioned areas. As the presence of steam is usual in the vast majority of reactions such as water gas shift, silica membranes used under wet conditions must be hydrothermally stable [17]. Unfortunately, silica membranes do not meet the requirement for hydrothermal stability since the silica structure collapses due to the further hydrolysis of the Si–O–Si framework caused by the physically adsorbed water on the surface [18,19], resulting in a deteriorated performance of the membranes, such as dramatic decrease of gas permeance and selectivity. Reducing the adsorption of water on the surface has been demonstrated to be effective in maintaining an intact structure for silica membranes [20]. The degree of water wettability is extremely critical for silica membranes and it is generally accepted that hydrophobic silica membranes exhibit more resistance to water attack than hydrophilic membranes [21].

A great deal of effort has been made in recent decades to reduce the water wettability, or to enhance the hydrophobic properties, of silica membranes. It has been reported that although both cobalt-doped silica and pure silica xerogels are hydrophilic, cobalt-doped silica adsorbs less amount of water than pure silica xerogel [22]. Tsuru et al. claimed that the improved hydrothermal stability of Co-doped silica membranes might be attributed to the surface chemistry, which reduces the attack of water vapor under hydrothermal conditions [23]. El-Feky et al. developed a hydrophobic silica membrane by cobalt-doping within the organic template silica matrix [24]. A more reliable strategy to reduce water wettability is modifying the silica membranes by replacing

* Corresponding author. Tel./fax: +86 10 67391536.
E-mail address: zrnie@bjut.edu.cn (Z.-R. Nie).

http://dx.doi.org/10.1016/j.memsci.2014.04.036
0376-7388/

the surface hydroxyl groups with hydrophobic groups via co-hydrolysis and condensation of tetraethyl orthosilicate (TEOS) and modified agents, normally, alkoxysilane with unhydrolyzed hydrophobic groups, for instance, methyltriethoxysilane (MTES) [20]. Since 1999, when the first work on hydrophobic silica membranes for gas separation was reported [20], a large number of organic groups have been used to modify silica membranes (xerogels) [25–29]. In our groups, silica membranes have been successfully modified by ethylene [21], methyl [30], trifluoropropyl [31] and phenyl [32], exhibiting a water contact angle (CA) larger than 100° and an outstanding hydrothermal stability. It can be seen from previous work that in order to enhance the hydrophobic property of silica membranes, a rather high concentration of alkoxysilane has to be used in the sol–gel process, for example, a MTES/TEOS molar ratio as high as 1 was employed in methyl-modified silica membranes [20], thus leading to a high cost for materials preparation since alkoxysilane is always very expensive. Therefore, decreasing the concentration of alkoxysilane in membrane preparation is of great significance from an economic point of view and it is one of our aims in the present work.

As a fluorocarbon chain, perfluorodecyl group has been proved to be significantly effective in reducing the water wettability of organic–inorganic hybrid silica membranes produced from silsesquioxane, 1,2-bis(triethoxysilyl)ethane (BTESE) [33]. A BTESE-derived silica membrane possesses a much more looser structure than TEOS-derived membranes due to the presence of ethylidene, instead of oxygen, linking to silicon atoms in the framework [34]; thus, TEOS seems to be more suitable for silica membrane preparation. To the best of our knowledge, TEOS-derived silica membranes modified by perfluorodecyl group have not yet been reported previously. In the present work, the influence of perfluorodecyl group modification on the wettability, pore structure, performance and long-term hydrothermal stability of TEOS-derived silica membranes is investigated in detail.

2. Experimental

2.1. Chemicals

Tetraethyl orthosilicate and 1H,1H,2H,2H-Perflouorodecyltriethoxysilane (PFDTES) were purchased from Alfa Aesar. Nitric acid (HNO_3) and ethanol (EtOH) were obtained from Beijing Chemical Works. Deionized water (H_2O) was produced by the water purification system (Ulupure, Chengdu, China). All chemicals were used as received without further purification.

2.2. Preparation of silica membranes

Perfluorodecyl-modified silica sols were prepared by the co-hydrolysis and condensation of TEOS and PFDTES under acidic conditions according to a final PFDTES/TEOS/EtOH/H_2O/HNO_3 moral ratio of x/1/7.6/6.4/0.085 (where x=0, 0.1, 0.2, 0.4 and 0.6). A mixture of HNO_3 and H_2O was added dropwise into a mixture of TEOS and EtOH with a moral ratio of 1/3.8 in an ice-bath under stirring. This mixture was refluxed under vigorous stirring at 60 °C for 2.5 h, followed subsequently by a slow addition of a mixture of PFDTES and EtOH with a moral ratio of x/3.8 (where x=0, 0.1, 0.2, 0.4 and 0.6). A clear sol was obtained after continuing stirring for 0.5 h and then the sol was diluted 19 times with EtOH for dip-coating.

Disc-shaped γ-Al_2O_3 membranes supported on macroporous α-Al_2O_3 ceramics were used as substrates for silica membranes. The silica membranes were deposited on the top of γ-Al_2O_3 membranes by carefully controlling the dip-coater(KSV, Finland) to contact the sol and move horizontally in a clean room (grade 100). After dip-coating, the samples were dried and then calcined at 400 °C for 4 h with a ramping rate of 0.5 °C/min. The dip-coating, drying and calcination procedure were repeated five times to reduce the surface defects. The residual sol was poured into a Petri dish, dried at room temperature and then calcined under the same condition as supported silica membranes, to obtain a xerogel for characterization. The pure silica membranes (xerogels) were denoted as SiO_2, and the modified ones as (xPFDTES)SiO_2, where x=0.1, 0.2, 0.4 and 0.6, respectively.

2.3. Characterization

The morphology of supported silica membranes was observed by a Quanta FEG 650 scanning electron microscope. The water contact angle was measured by a Dataphysics OCA20 video-based contact angle system. A water droplet of 2 μL was injected on the membrane surface with a rate of 2 μL/s. Infrared spectra were carried out on a Nicolet 5700 FT-IR apparatus using the xerogel powder diluted with potassium bromide (KBr) pellets. Solid state ^{29}Si magic angle spinning nuclear magnetic resonance (^{29}Si MAS NMR) spectra were collected on a Bruker AV300 spectrometer under the following conditions: 5 mm MAS probe, 59.62 MHz resonance frequency, $\pi/2$ pulse, 6.0 μs pulse width, 5 kHz magic-angle spin, 600 s delay time and 200 scans. Chemical shifts were referenced to tetramethysilane (TMS) at 0 ppm. Nitrogen adsorption measurement was performed at −196 °C on a Micromeritics ASAP 2020M volumetric adsorption analyzer. Before measurement, the samples were outgassed under vacuum at 300 °C for 72 h to remove the physically adsorbed water and impurities. The pore size distribution was calculated based on the Saito–Foley modified Horváth–Kawazoe method using the physical parameters applicable to microporous silica materials.

2.4. Gas permeation and separation

The single gas (H_2,CO_2 and SF_6) permeation of supported silica membranes was measured with a dead-end setup. Membranes were sealed in a stainless steel module using high-temperature-resistant graphite O-rings with the silica separation layer exposed to the feed side and the substrate to atmosphere (the permeate side). The gas pressure of the feed side was adjusted by a gas regulator valve and the differential pressure was maintained at 100 kPa. The gas flux was recorded by an electronic gas mass flow meter (Alicat) or a soap bubble flow meter in the case of hydrothermal stability measurement discussed afterwards.

The binary gas separation (H_2/CO_2) was determined by the method reported previously [31]. The feed side was exposed to atmosphere and the permeate side was connected to a gas chromatograph (GC-2014,Shimadzu) using a carbon molecular sieve column with a thermal conductor (TCD). A binary gas mixture, where the flux of H_2 and CO_2 (a total flux of 50 mL/min with a H_2/CO_2 ratio of 1:2 in this case) was precisely controlled by gas mass flow controllers (Alicat), was introduced to the feed side and at the permeate side Argon (Ar, 300 mL/min) was used as sweep gas to carry the permeate gases into GC for concentration analysis. The separation factor (α) of a binary gas mixture is calculated from the gas concentration (c_{feed} and $c_{permeate}$) at the feed and permeate sides using the following equation:

$$\alpha = \frac{c_{H_2,permeate}}{c_{CO_2,permeate}} \frac{c_{CO_2,feed}}{c_{H_2,feed}} \quad (1)$$

2.5. Hydrothermal stability

A home-made device as illustrated in Fig. 1 was used to measure the hydrothermal stability of silica membranes. To create

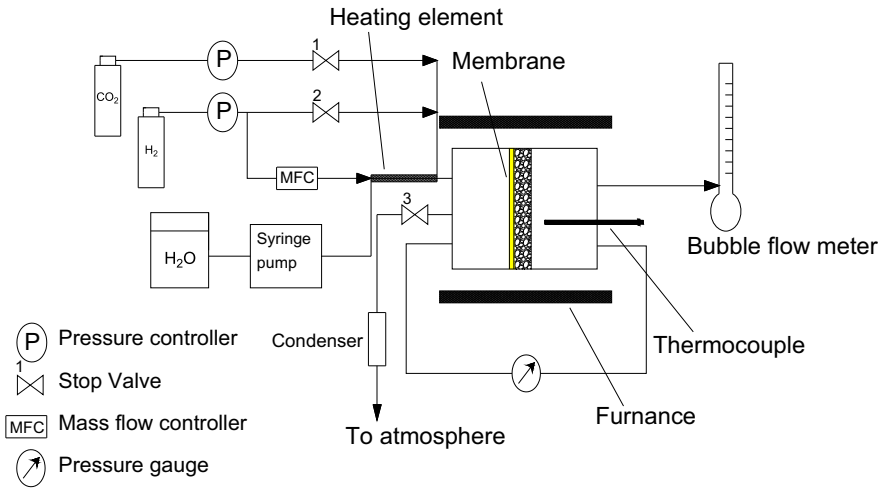

Fig. 1. Schematic diagram of the experimental setup for hydrothermal stability measurement.

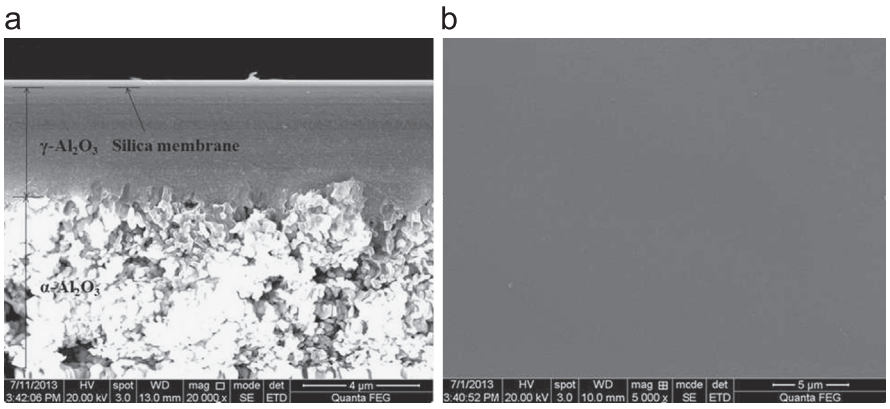

Fig. 2. SEM images of the supported (0.2PFDTES)SiO_2 silica membranes. (a) cross-section and (b) surface.

a humid atmosphere, a certain amount of water was vaporized at a temperature higher than 100 °C and then the steam, carried by hydrogen with a flux of 47.5 mL/min, was introduced to the surface of the silica separation layer. The flux of water and hydrogen was precisely controlled by a syringe pump and a gas mass flow controller, respectively, and the steam accounted for 5 mol% of the total flux. The temperature of membranes was maintained at 250 °C. A single gas permeation of H_2 and CO_2 was measured after the membranes had been exposed to humid atmosphere for a certain time. The hydrothermal stability of membranes was evaluated by the variation of hydrogen permeance and H_2/CO_2 permselectivity at different exposed times.

3. Results and discussion

3.1. Morphology

Fig. 2 shows a SEM micrograph of the profile of silica membranes. It can be clearly observed that a silica membrane, with a thickness of about 250 nm, has been successfully deposited on the γ-Al_2O_3/α-Al_2O_3 substrates (Fig. 1a). No distinct pinholes and cracks are observed on the surface of top layer (Fig. 1b); however, permeation with a large size gas, for instance, SF_6, is more appropriate to detect whether there are obnoxious defects in the top layer, due to the limitation of the magnification of a scanning electron microscope.

3.2. Wettability of silica membranes

The wettability of silica membranes can be characterized by the water contact angle measured on a video-based contact angle system. Fig. 3 exhibits the profile of a water droplet on the surface of supported silica membranes. The angle formed between the liquid/solid interface and the liquid/vapor interface is the contact angle. The silica membranes become hydrophobic after modification, with a considerably larger water contact angle than pure membranes (Fig. 3a), indicating that the wettability of the modified membranes has been dramatically reduced. In comparison with the results reported previously, perfluorodecyl modification is proved to be more liable to enhance the hydrophobic property of membranes compared to other groups. For example, a very low concentration of perfluorodecyl group (molar ratio PFDTES/TEOS = 0.2, Fig. 3c) leads to a hydrophobic silica membrane with a water contact angle of $112.6 \pm 0.5^\circ$, much higher than those membranes modified with a trifluoropropyl group [31], an ethylene group [21] and phenyl groups [32] at the same or higher concentration of alkoxysilane in the mixture (alkoxysilane/TEOS ≤ 0.4). This observation might be attributed to the possibility that perfluorodecyl groups generate a rougher surface for the membranes than other groups because perfluorodecyl groups have a much longer chain. However, steric hindrance derived from the long chains also prevents perfluorodecyl groups from further replacing hydroxyl groups at a higher PFDTES/TEOS molar ratio. This can be demonstrated by the fact that a further increase of PFDTES/TEOS molar ratio to 0.4 results in only a slight increase of

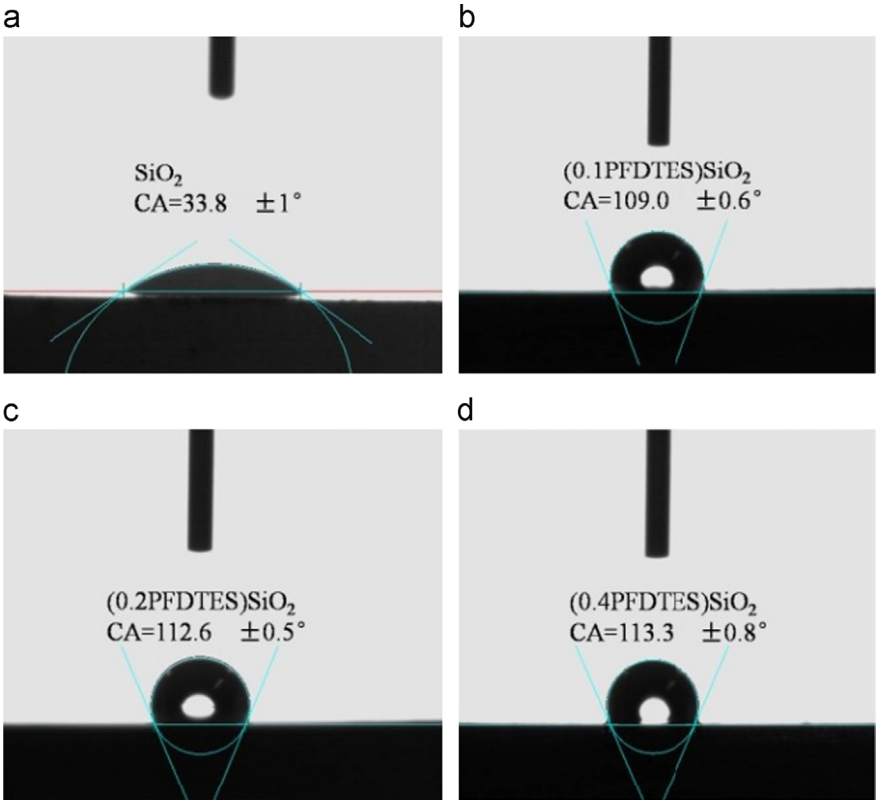

Fig. 3. Shape of a water droplet on the surface of supported silica membranes.

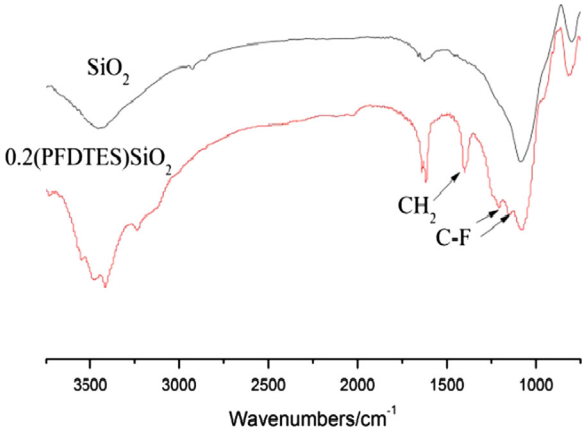

Fig. 4. FT-IR spectra of pure and (0.2PFDTES)SiO_2 silica membranes.

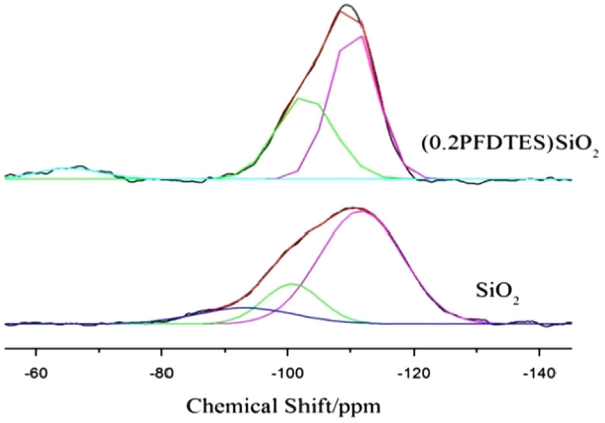

Fig. 5. Solid state ^{29}Si MAS NMR spectra of the pure and (0.2PFDTES)SiO_2 silica membranes.

the water contact angle (Fig. 3d). A reduced concentration of alkoxysilane used in this work is beneficial to decrease the cost of materials synthesis.

Chemical bonding of silica and functional groups is investigated using FT-IR spectra shown in Fig. 4. The band at 1400 cm^{-1} corresponds to the wagging vibration of $-CH_2-$, and the absorption peaks at 1149 cm^{-1} and 1208 cm^{-1} can be assigned to the vibration of C–F. These bands are observed in the spectra of the modified membranes but absent in the pure silica membranes, indicating that perfluorodecyl groups have been successfully incorporated into silica membranes and remain undamaged even after calcination at 400 °C. The band at 1079 cm^{-1} in both modified and pure silica membranes can be attributed to the asymmetric stretching vibration of Si–O–Si, and the presence of this band indicates an intact silica network.

The presence of perfluorodecyl group in silica membranes can be further confirmed by solid state ^{29}Si MAS NMR. The spectra of the pure silica membranes and modified sample (0.2PFDTES)SiO_2, fitted by the Gaussian approach, are shown in Fig. 5. For all silica membranes, the resonances at a chemical shift of −112 and −100 ppm are assigned to the silicon atoms $Q^4[Si(OSi)_4]$ and $Q^3[Si(OSi)_3(OH)]$, respectively. An additional weak resonance related to the silicon atoms $T^3[Si(OSi)_3R$, R=perfluorodecyl group] is observed at a chemical shift of −65 ppm for the modified sample. The relative amount (mol%) of different types of silicon atoms can be quantitatively calculated by integrating the Q^m and T^n resonances and the results are listed in Table 1. The absolute values (mmol/g) for the hydroxyl and perfluorodecyl groups in silica membranes can be calculated according to the following

Table 1
Solid state ^{29}Si MAS NMR results of the pure and (0.2PFDTES)SiO_2 silica membranes.

Membranes	Q^4 (mol%)	Q^3 (mol%)	Q^2 (mol%)	T^3 (mol%)	T^2 (mol%)	[OH] (mmol g^{-1})	[$C_2H_4C_8F_{17}$] (mmol g^{-1})
SiO_2	70.76	17.42	11.82	–	–	6.45	–
(0.2PFDTES)SiO_2	55.82	38.55	–	5.63	–	4.37	0.64

formula (1 mol silica membrane is used for calculation):

$$[OH]_{SiO_2} = \frac{I_{Q^3} + 2 \times I_{Q^2}}{60 \times I_{Q^4} + 69 \times I_{Q^3} + 78 \times I_{Q^2}} 1000 \quad (2)$$

$$[OH]_{(0.2PFDTES)SiO_2} = \frac{I_{Q^3}}{60 \times I_{Q^4} + 69 \times I_{Q^3} + 499 \times I_{T^3}} 1000 \quad (3)$$

$$[C_2H_4C_8F_{17}]_{(0.2PFDTES)SiO_2} = \frac{I_{T^3}}{60 \times I_{Q^4} + 69 \times I_{Q^3} + 499 \times I_{T^3}} 1000 \quad (4)$$

In the formula, the item I means the molar concentration (mol%) of Q^n (n=2–4) and T^m (m=2–3) species, the denominator represents the molecular mass (g/mol) of silica membranes and the numerator is the molar percentage of hydroxyl or the perfluorodecyl group.

It can be seen from Table 1 that for the modified samples, the concentration of perfluorodecyl group is 0.64 mmol/g, and the concentration of surface hydroxyl groups decreases from 6.45 mmol/g to 4.37 mmol/g. The presence of perfluorodecyl groups and the decreased amount of hydroxyl groups are responsible for the languishment of water wettability of modified silica membranes. Furthermore, the absence of Q^2[$Si(OSi)_2(OH)_2$] signal at the chemical shift of −90 ppm and T^2[$Si(OSi)_2(OH)R$, R=perfluorodecyl group] signal at −53 ppm in the modified samples indicates a high condensation degree of the PFDTES and TEOS in the so–gel process, which makes the amount of surface hydroxyl groups as small as possible [35]. The relatively weaker resonance of T^3 atoms compared with those reported in a previous work [21,31] is ascribed to the less amount of alkoxysilane used in this work.

3.3. Pore structure of xerogel

On the one hand perfluorodecyl modification can enhance the hydrophobicity of silica membranes, but on the other it will have an influence on the pore structure of the resultant materials. The amount of PFDTES in the mixture is the most critical factor which decides the pore structure of silica membranes. Fig. 6 shows the N_2 adsorption of silica xerogels modified with different concentrations of PFDTES. All samples except (0.6PFDTES)SiO_2 exhibit a type I isotherm with a sharp increase of N_2 adsorption at low relative pressure ($P/P_0 < 0.01$) and a saturated adsorption at approximately $P/P_0 > 0.1$, indicative of a typical characteristic for microporous materials. A type IV isotherm is observed for the sample (0.6PFDTES)SiO_2, suggesting that the sample is predominantly mesoporous and not applicable for gas separation. For microporous membranes, it is reasonable to expect that the introduction of perfluorodecyl groups on the silica surface gives rise to a decreased amount of nitrogen adsorption and the more amount of perfluorodecyl groups is incorporated, the less quantity of nitrogen adsorption occurs because perfluorodecyl groups tend to occupy a certain proportion of pore space in the samples. This is confirmed by the isotherms in Fig. 6, but it seems to be abnormal that the amount of nitrogen adsorption for the sample (0.1PFDTES)SiO_2 is much less than those of samples with a higher concentration of perfluorodecyl groups. This phenomenon might be related

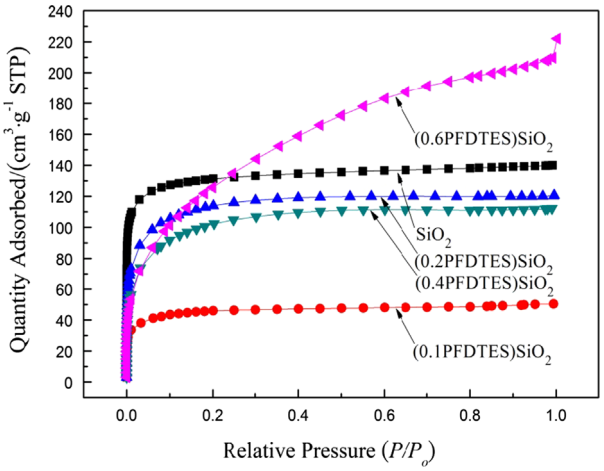

Fig. 6. N_2 adsorption isotherms of pure and modified silica xerogels.

to the pore formation mechanism of silica xerogels (Fig. 7). It is generally accepted that clusters are generated during the co-hydrolysis and condensation processes of TEOS and other silanes, particularly under acidic conditions [36]. The clusters would be low branched or highly branched depending on the amount of long chains of silane in the reactant mixtures. The interpenetration of low branched clusters leads to a much lower porosity, in other words, a denser structure, because during interpenetration the branches of one cluster insert into and occupy the space between the branches of other clusters. However, for the highly branched clusters, they are apt to aggregate to form a relatively looser microporous structure. Therefore, the pore volume of xerogel depends on the degree of interpenetration of low branched clusters and the aggregation of highly branched clusters. As shown in Fig. 7, it can be expected that the amount of low branched clusters (Fig. 7a) is produced much more than that of highly branched clusters (Fig. 7b) at a low PFDTES/TEOS molar ratio (such as 0.1) due to the presence of a smaller amount of long-chain perfluorodecyl groups. In this case, the interpenetration of low branched clusters occurs much more frequently than the aggregation of highly branched clusters, leading to a lower porosity (Fig. 7c). With the increase of PFDTES concentration, the co-hydrolysis and condensation of precursors result in much more highly branched clusters than low branched clusters; thus the aggregation of highly branched clusters predominates over the interpenetration of low branched clusters, bringing about a higher pore volume (Fig. 7d). When the PFDTES/TEOS molar ratio further increases to 0.6, non-fractal particles rather than fractal branched clusters are developed and the agglomeration of these particles is inclined to generate much larger pores (mesopores) [37]. Taking account of both hydrophobic property and pore structure, the sample (0.2PFDTES)SiO_2 is preferred to be used for performance assessment.

Fig. 8 shows the pore size distribution of silica xerogels with a PFDTES/TEOS molar ratio less than 0.6. As can be seen, the silica xerogels exhibit a pore size ranging from 0.45 to 0.9 nm, regardless

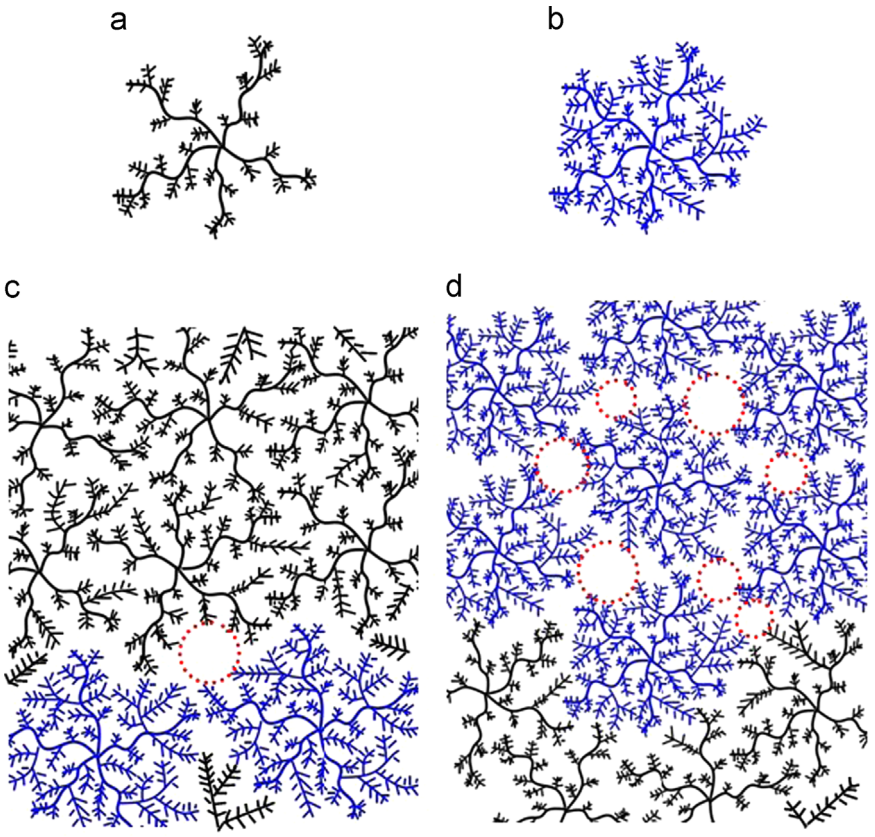

Fig. 7. Schematic diagram of the formation mechanism of micropores in silica xerogels: (a) low branched clusters; (b) highly branched clusters; (c) the predominant interpenetration of low branched clusters leading to a lower porosity and (d) the predominant aggregation of highly branched clusters resulting in a higher pore volume. The circles in (c) and (d) represent the micropores.

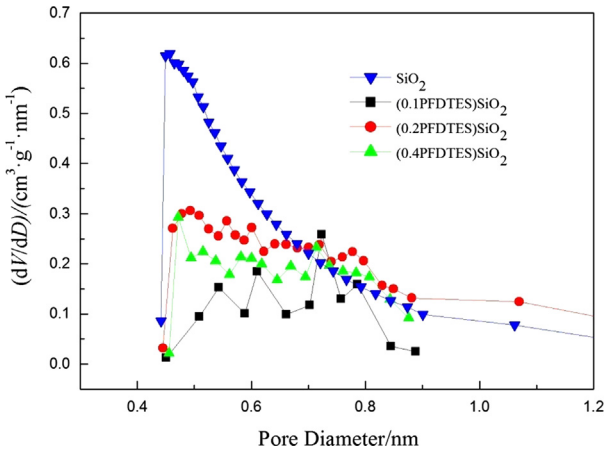

Fig. 8. Pore size distributions of pure and modified silica xerogels.

of whether the samples have been modified with perfluorodecyl groups, suggesting that the novel materials can be used for molecular sieving applications. The surface area and pore volume of the materials are listed in Table 2. It can be seen from Table 2 that perfluorodecyl modification leads to a decrease of the surface area and pore volume except for the sample (0.6PFDTES)SiO_2.

3.4. Silica membranes performance

Temperature dependence of single gas (H_2, CO_2 and SF_6) permeance for supported silica membranes (0.2PFDTES)SiO_2 and the permselectivity of H_2/CO_2 are listed in Tables 3 and 4,

Table 2
Pore structure parameter of pure and modified silica xerogels.

Sample	BET surface area/$m^2\ g^{-1}$	Pore volume/$cm^3\ g^{-1}$
SiO_2	444.24	0.22
(0.1PFDTES)SiO_2	157.96	0.08
(0.2PFDTES)SiO_2	359.62	0.17
(0.4PFDTES)SiO_2	336.59	0.16
(0.6PFDTES)SiO_2	477.73	0.32

respectively. As seen, the permeance of H_2 increases remarkably as the temperature rises from 100 to 300 °C, but in contrast, that of CO_2 decreases very slightly with increasing temperatures. A permeance of SF_6 is also observed, indicating the presence of pores with a kinetic diameter larger than 0.55 nm, as shown in the pore size distribution curves of Fig. 8, or the existence of surface defects formed during the dip-coating and calcination process, which are invisible in the images of Fig. 1 due to the limited magnification of SEM devices. A dominant Knudsen diffusion for the transport of non-condensable SF_6 molecules in the membranes can be confirmed by the fact that SF_6 permeance decreases with increasing temperatures, a typical characteristic for Knudsen diffusion.

The gas transport mechanism for H_2 and CO_2 seems to be much more complex than SF_6. For H_2, a combination of thermally activated surface diffusion and Knudsen diffusion may occur. The dramatic increase of H_2 permeance with increasing temperatures and the H_2/CO_2 permselectivity higher than that of Knudsen diffusion (H_2/CO_2=4.69) indicate that H_2 molecules move through the membranes according to an activated diffusion, but the presence of pores or defects much larger than the kinetic diameter

Table 3
Temperature dependence of single gas permeance ($\times 10^{-7}$ mol m^{-2} s^{-1} Pa^{-1}) for supported silica membranes (0.2PFDTES)SiO_2.

Gas	100 °C	150 °C	200 °C	250 °C	300 °C
H_2	7.13	7.9	8.76	9.3	9.71
CO_2	1.47	1.4	1.35	1.37	1.35
SF_6	0.51	0.46	0.42	0.39	0.37

Table 4
Temperature dependence of permselectivity and binary gas separation factor of H_2/CO_2 for supported silica membranes (0.2PFDTES)SiO_2.

	100 °C	150 °C	200 °C	250 °C	300 °C
Permselectivity	4.85	5.64	6.49	6.79	7.19
Separation factor	3.90	7.14	8.70	10.07	12.11

of H_2 suggests that Knudsen diffusion through the pore channels is also responsible for H_2 transport. Due to the large polarity of hydroxyl groups and perfluorodecyl groups on the surface, CO_2 molecules easily adsorb on the pore surface, and as a result, move through the membranes based on thermally activated surface diffusion. However, the temperature dependence of CO_2 permeance does not comply with an activated surface diffusion, which shows a permeance positively correlated with temperatures. This observation may be caused by the possibility that in addition to activated surface diffusion, Knudsen diffusion may also take place for CO_2 molecules, which can be demonstrated by the 'Knudsen like' temperature dependence of CO_2 permeance as shown in Table 3. In fact, it is really reasonable that pores or defects larger than the kinetic diameter of SF_6 can act as a path for Knudsen diffusion [38].

To investigate the activated surface diffusion of H_2 and CO_2 in silica membranes, gas permeance associated with Knudsen diffusion should be subtracted from the total permeance, and the results are listed in Table 5. It is generally accepted that for Knudsen diffusion, the selectivity is equal to the inverse ratio of the square root of the molecular weight of the two permeating gases. For instance, in the case of H_2 and SF_6, the heavier SF_6 permeates slower than H_2 by the factor $(146/2)^{1/2}=8.54$, and for CO_2/SF_6, the selectivity is $(146/44)^{1/2}=1.82$. Therefore, the H_2 and CO_2 permeances related to Knudsen diffusion can be obtained from SF_6 permeance. The Arrhenius fit of the gas permeance of silica membranes after Knudsen diffusion subtraction is shown in Fig. 9. The transport rate can be expressed in terms of a modified Fick's law as follows:

$$F = F_0 \exp\left(-\frac{E_a}{RT}\right) \quad (5)$$

Here F is the gas permeance, E_a is the apparent activation energy, and F_0 is a temperature-independent parameter. To assess the ability of a gas molecule diffusing along the surface, an effective activated energy, E_m, representing the energy barrier between two adjacent sorption sites, is put forward. Additionally, the isosteric heat of adsorption, Q_{st}, should also be taken into account. It has been verified that the effective activated energy is the sum of the apparent activated energy and the isosteric heat of adsorption [39]:

$$E_m = E_a + Q_{st} \quad (6)$$

The apparent activated energy for the permeance of the various gases can be calculated by fitting the natural log of permeance over the inverse of temperature (Fig. 9). The isosteric heat of adsorption for H_2 and CO_2 of silica materials has been previously

Table 5
Temperature dependence of single gas permeance ($\times 10^{-7}$ molm^{-2}s^{-1}Pa^{-1}) for supported silica membranes (0.2PFDTES)SiO_2 after subtraction of Knudsen diffusion.[a]

Gas	100 °C	150 °C	200 °C	250 °C	300 °C
H_2	2.81 (60.6)	4.01 (49.2)	5.21 (40.5)	5.95 (36.0)	6.53 (32.7)
CO_2	0.55 (62.6)	0.57 (59.3)	0.59 (56.3)	0.66 (51.8)	0.67 (50.4)

[a] The data in brackets are the contribution of Knudsen diffusion to the total permeance (%).

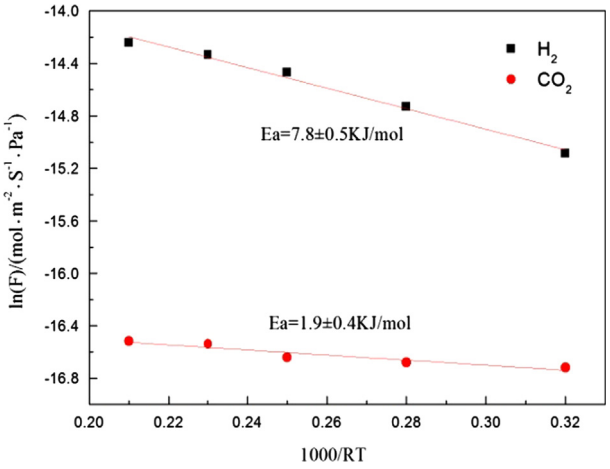

Fig. 9. Arrhenius plots of the gas permeance of (0.2PFDTES)SiO_2 membranes after subtraction of Knudsen diffusion.

reported as 6 and 24 kJ/mol, respectively [39], but those for perfluorodecyl-modified silica membranes remain unclear. Therefore, the exact effective activated energy for H_2 and CO_2 in perfluorodecyl-modified silica membranes is difficult to be determined. It can be seen from Table 5 that CO_2 molecules are more difficult to go through modified silica membranes by thermally activated surface diffusion than H_2. This observation implies the higher energy barrier for CO_2 than H_2, and the effective activated energy for CO_2 can be roughly estimated to be higher than that for H_2 in perfluorodecyl-modified silica membranes. It is also demonstrated in Table 5 that the relative contribution of Knudsen diffusion increases with decreasing temperature and even becomes dominant for both H_2 and CO_2 at sufficiently low temperatures, for instance, <100 °C. This observation can be explained by the fact that Knudsen diffusion is proportional to $T^{-0.5}$ (T represents Kelvin temperature) [38]. From Table 5, it is also easy to deduce that thermally activated surface diffusion becomes predominant at higher temperatures (>200 °C) for H_2, but it is not the case for CO_2, and that is why the H_2/CO_2 permselectivity is larger than that of the Knudsen diffusion. At such a high temperature, CO_2 molecules move through the membranes with a speed higher than that of thermally activated surface diffusion; consequently, the H_2/CO_2 permselectivity would not be very high even at a high temperature of 300 °C (in this case it is 7.19, only slightly higher than that of Knudsen diffusion). Although the H_2/CO_2 permselectivity seems to be relatively lower than those of previous work [40] and not sufficient for industrial applications [41], the modified silica membranes in this work exhibit a high H_2 permeance of 9.71×10^{-7} mol m^{-2} s^{-1} Pa^{-1}, much larger than those reported in recent literature [14,42].

The separation factor of binary H_2/CO_2 mixture is shown in Table 4, larger than the permselectivity except for at 100 °C. It is of great significance because in industrial applications the performance of membranes should be evaluated based on binary or multicomponent gas separation. The transport mechanism of gas

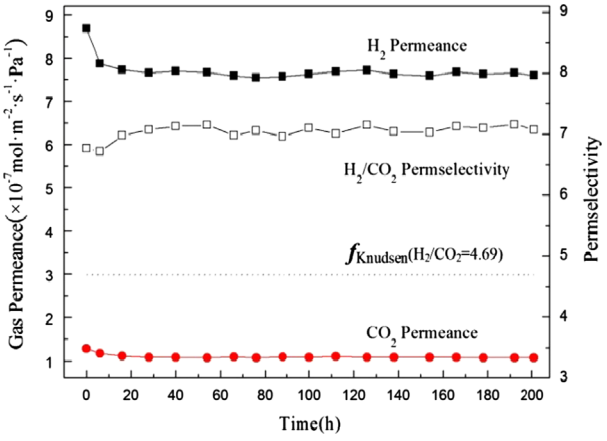

Fig. 10. Time course of single gas permeance and H_2/CO_2 permselectivity of the supported (0.2PFDTES)SiO_2 silica membrane after being exposed to humid atmosphere.

molecules in the mixture may be different from that in single gas since the interaction (collision) of gas molecules should be taken into account. It has been proved that the adsorption of CO_2 near the entrance of the micropores on the surface of silica membranes is decreased due to the collision of H_2 molecules present in the gas mixture [43] and therefore the pore blocking owing to CO_2 adsorption does not occur severely. Driven by the pressure difference derived from the sweep gas, H_2 molecules move together with CO_2 molecules along the channels of micropores toward the permeate side. The collision from CO_2 molecules makes H_2 molecules move much faster due to the considerably lower molecular mass of H_2 than CO_2, thus resulting in a relatively higher H_2/CO_2 separation factor. Of course, a molecular sieving mechanism is also responsible for the separation of the H_2/CO_2 mixture.

The supported silica membrane (0.2PFDTES)SiO_2 is exposed to a humid atmosphere at 250 °C for a certain time and then the single gas permeance and H_2/CO_2 permselectivity are measured to reveal the long-term hydrothermal stability. The result is exhibited in Fig. 10. The H_2 permeance exhibits a slight decrease of 9.3% after being exposed to a humid atmosphere for 6 h and then remains almost constant for at least 200 h, in stark contrast to pure silica membranes whose permeance decreases sharply (by as much as 50% or greater) within the first few hours after steam exposure [44–47]. A H_2/CO_2 permselectivity of approximately 7 is maintained during the measurement. The stable H_2 permeance and H_2/CO_2 permselectivity suggest that the modified silica membranes possess a high hydrothermal stability compared to the pure silica membranes. The improvement of hydrothermal stability can be attributed to the decrease of water wettability, which has been proved to be advantageous to maintain an intact microporous structure for silica membranes [31].

4. Conclusion

Perfluorodecyl groups have been successfully incorporated into silica membranes by the acid-catalyzed co-hydrolysis and condensation of tetraethyl orthosilicate (TEOS) and 1H,1H,2H,2H-Perflouorodecyltriethoxysilane (PFDTES), and the supported perfluorodecyl-modified silica membranes have been obtained by dip-coating the sol on γ-Al_2O_3/α-Al_2O_3 substrates under clean room conditions. The incorporation of perfluorodecyl groups considerably reduces the water wettability of silica membranes, with a water contact angle of $112.6 \pm 0.5^\circ$ at a PFDTES/TEOS molar ratio of 0.2. A pore size ranging from 0.45 to 0.9 nm is observed at such a PFDTES concentration. The hydrogen permeance increases with increasing temperatures and reaches a value of 9.71×10^{-7} mol m^{-2} s^{-1} Pa^{-1} at 300 °C. At such a temperature, the H_2/CO_2 permselectivity and binary gas separation factor are 7.19 and 12.11 at 300 °C, respectively. The modified silica membranes are highly hydrothermally stable under a humid condition with a temperature of 250 °C and a water vapor molar ratio of 5%, showing a great potential in applications such as water gas shift reaction where a large amount of steam is present and mixed gas separation is required.

Acknowledgment

This research was financially supported by the National Natural Science Foundation of China (Grant nos. 21171014 and 50502002), the National High Technology Research and Development Program for Advanced Materials of China (Grant no. 2009AA03Z213) and the Scientific Research Common Program of the Beijing Municipal Commission of Education (Grant no. KZ201410005006).

References

[1] S. Araki, H. Miyanishi, H. Yano, S. Tanaka, Y. Miyake, Water gas shift reaction in a membrane reactor using a high hydrogen permselective silica membrane, Sep. Sci. Technol. 48 (2013) 76–83.
[2] J.C. Diniz da Costa, G.P. Reed, K. Thambimuthu, High temperature gas separation membranes in coal gasification, Energy Proc. 1 (2009) 295–302.
[3] S.-J. Kim, S.W. Yang, G.K. Reddy, P. Smirniotis, J.H. Dong, Zeolite membrane reactor for high-temperature water-gas shift reaction: effects of membrane properties and operating Conditions, Energy Fuels 27 (2013) 4471–4480.
[4] B. Dittmar, A. Behrens, N. Schodel, M. Ruttinger, T. Franco, G. Straczewski, R. Dittmeyer, Methane steam reforming operation and thermal stability of new porous metal supported tubular palladium composite membranes, Int. J. Hydrogen Energy 38 (2013) 8759–8771.
[5] M. Saric, Y.C. van Delft, R. Sumbharaju, D.F. Meyer, A. de Groot, Steam reforming of methane in a bench-scale membrane reactor at realistic working conditions, Catal. Today 193 (2012) 74–80.
[6] R. Molinari, P. Argurio, S.M. Carnevale, T. Poerio, Membrane contactors operating in mild conditions for liquid phase partial oxidation of methane, J. Membr. Sci. 366 (2011) 139–147.
[7] L. Chibane, B. Djellouli, Y. Benguerba, Forced composition cycling of a Pd-membrane reactor for pure hydrogen production from the reaction of partial oxidation of methane, Chem. Eng. J. 178 (2011) 398–406.
[8] N. Jullok, R. Martinez, C. Wouters, P. Luis, M.T. Sanz, B. van der Bruggen, A biologically inspired hydrophobic membrane for application in pervaporation, Langmuir 29 (2013) 1510–1516.
[9] X.L. Dong, Y.S. Lin, Synthesis of an organophilic ZIF-71 membrane for pervaporation solvent separation, Chem. Commun. 49 (2013) 1196–1198.
[10] D.K. Wang, J. Motuzas, J.C.D. da Costa, S. Smart, Rapid thermal processing of tubular cobalt oxide silica membranes, Int. J. Hydrogen Energy 38 (2013) 7394–7399.
[11] V. Durand, M. Drobek, M. Duchateau, A. Hertz, J.-C. Ruiz, S. Sarrade, C. Guizard, A. Julbe, Potential of sub-and supercritical CO_2 reaction media for sol–gel deposition of silica-based molecular sieve membranes, Sep. Purif. Technol. 121 (2013) 30–37.
[12] M. Kanezashi, D. Fuchigami, T. Yoshioka, T. Tsuru, Control of Pd dispersion in sol–gel-derived amorphous silica membranes for hydrogen separation at high temperatures, J. Membr. Sci. 439 (2013) 78–86.
[13] J.H. Wang, G.H. Gong, M. Kanezashi, T. Yoshioka, K. Ito, T. Tsuru, Pervaporation performance and characterization of organosilicamembranes with a tuned pore size by solid-phase HCl post-treatment, J. Membr. Sci. 441 (2013) 120–128.
[14] S. Smart, J.F. Vente, J.C.D. da Costa, High temperature H_2/CO_2 separation using cobalt oxide silica membranes, Int. J. Hydrogen Energy 37 (2012) 12700–12707.
[15] J.H. Wang, T. Tsuru, Cobalt-doped silica membranes for pervaporation dehydration of ethanol/water solutions, J. Membr. Sci. 369 (2011) 13–19.
[16] M.W.J. Luiten, N.E. Benes, C. Huiskes, H. Kruidhof, A. Nijmeijer, Robust method for micro-porous silica membrane fabrication, J. Membr. Sci. 348 (2010) 1–5.
[17] S. Battersby, S. Smart, B. Ladewig, S.M. Liu, M.C. Duke, V. Rudolph, J.C.D. da Costa, Hydrothermal stability of cobalt silica membranes in a water gas shift membrane reactor, Sep. Purif. Technol. 66 (2009) 299–305.
[18] M.C. Duke, J.C.D. da Costa, D.D. Do, P.G. Gray, G.Q. Lu, Hydrothermally robust molecular sieve silica for wet gas separation, Adv. Funct. Mater. 16 (2006) 1215–1220.
[19] H.L. Castricum, A. Sah, R. Kreiter, D.H.A. Blank, J.F. Vente, J.E. ten Elshof, Hybrid ceramic nanosieves: stabilizing nanopores with organic links, Chem. Commun. (2008) 1103–1105.

[20] R.M. de Vos, W.F. Maier, H. Verweij, Hydrophobic silica membranes for gas separation, J. Membr. Sci. 158 (1999) 277–288.
[21] Q. Wei, Y.-L. Wang, Z.-R. Nie, C.-X. Yu, Q.-Y. Li, J.-X. Zou, C.-J. Li, Facile synthesis of hydrophobic microporous silica membranes and their resistance to humid atmosphere, Microporous Mesoporous Mater. 111 (2008) 97–103.
[22] D. Uhlmanna, S.M. Liu, B.P. Ladewig, J.C.D. da Costa, Cobalt-doped silica membranes for gas separation, J. Membr. Sci. 326 (2009) 316–321.
[23] R. Igi, T. Yoshioka, Y.H. Ikuhara, Y. Iwamoto, T. Tsuru, Characterization of Co-doped silica for improved hydrothermal stability and application to hydrogen separation membranes at high temperatures, J. Am. Ceram. Soc. 91 (2008) 2975–2981.
[24] H.H. El-feky, K. Briceño, E. de, O. Jardim, J.S. Albero, T. Gumi, Novel silica membrane material for molecular sieve applications, Microporous Mesoporous Mater. 179 (2013) 22–29.
[25] Y.V. Kazakevich, A.Y. Fadeev, Adsorption characterization of oligo(dimethylsiloxane)-modified silicas: an example of highly hydrophobic surfaces with non-aliphatic architecture, Langmuir 18 (2002) 3117–3122.
[26] P.B. Wagh, S.V. Ingale, Comparison of some physico-chemical properties of hydrophilic and hydrophobic silica aerogels, Ceram. Int. 28 (2002) 43–50.
[27] A.V. Rao, M.M. Kulkarni, Effect of glycerol additive on physical properties of hydrophobic silica aerogels, Mater. Chem. Phys. 77 (2003) 819–825.
[28] H.E. Rassy, P. Buisson, B. Bouali, A. Perrard, A.C. Pierre, Surface characterization of silica aerogels with different proportions of hydrophobic groups, dried by the CO_2 supercritical method, Langmuir 19 (2003) 358–363.
[29] H.E. Rassy, A.C. Pierre, NMR and IR spectroscopy of silica aerogels with different hydrophobic characteristics, J. Non-Cryst. Solids 351 (2005) 1603–1610.
[30] C.-X. Yu, Q. Wei, Y.-L. Wang, Q.-Y. Li, Z.-R. Nie, J.-X. Zou, Preparation and Characterization of hydrophobic mesoporous silica membranes, Chin. J. Inorg. Chem. 23 (2006) 957–962.
[31] Q. Wei, F. Wang, Z.-R. Nie, C.-L. Song, Y.-L. Wang, Q.-Y. Li, Highly hydrothermally stable microporous silica membranes for hydrogen separation, J. Phys. Chem. B 112 (2008) 9354–9359.
[32] Z.-J. Li, Q. Wei, N.-N. Wei, Q.-Y. Li, Z.-R. Nie, Preparation and characterization of hydrophobic microporous silica membranes modified by phenyl groups, Chem. J. Chin. Univ. 31 (2010) 2482–2487.
[33] L. Song, Q. Wei, R.-Q. Hao, Z.-R. Nie, Q.-Y. Li, Preparation and gas separation of organic-inorganic hybrid silica membranes modified by perfluorodecyl group, Chem. J. Chin. Univ. 33 (2012) 1670–1675.
[34] M. Kanezashi, K. Yada, T. Yoshioka, T. Tsuru, Design of silica networks for development of highly permeable hydrogen separation membranes with hydrothermal stability, J. Am. Chem. Soc. 131 (2009) 414–415.
[35] D.J. Yang, J.P. Li, Y. Xu, D. Wu, Y.H. Sun, H.Y. Zhu, F. Deng, Direct formation of hydrophobic silica-based micro/mesoporous hybrids from polymethylhydrosiloxane and tetraethoxysilane, Microporous Mesoporous Mater. 95 (2006) 180–186.
[36] C.J. Brinker, R. Sehgal, S.L. Hietala, R. Deshpande, D.M. Smith, D. Loy, C. S. Ashley, Sol–gel strategies for controlled porosity inorganic materials, J. Membr. Sci. 94 (1994) 85–102.
[37] A.J. Burggraaf, L. Cot, Fundamentals of Inorganic Membrane Science and Technology, Elsevier, Amsterdam, Lausanne, New York, Oxford, Shannon, Tokyo, 1996.
[38] V. Boffa, D.H.A. Blank, J.E. ten Elshof, Hydrothermal stability of microporous silica and niobia–silica membranes, J. Membr. Sci. 319 (2008) 256–263.
[39] R.M. de Vos, H. Verweij, Improved performance of silica membranes for gas separation, J. Membr. Sci. 143 (1998) 37–51.
[40] H. Qi, H.R. Chen, L. Li, G.Z. Zhu, N.P. Xu, Effect of Nb content on hydrothermal stability of a novel ethylenebridgedsilsesquioxane molecularsievingmembraneforH$_2$/CO_2 separation, J. Membr. Sci. 421–422 (2012) 190–200.
[41] H.F. Qureshi, A. Nijmeijer, L. Winnubst, Influence of sol–gel process parameters on the micro-structure and performance of hybrid silica membranes, J. Membr. Sci. 446 (2013) 19–25.
[42] V. Boffa, J.E. ten Elshof, A.V. Petukhov, D.H.A. Blank, Microporous niobia–silica membrane with very low CO_2 permeability, ChemSusChem 1 (2008) 437–443.
[43] Y.-S. Kim, K. Kusakabe, S. Morooka, S.-M. Yang, Preparation of microporous silica membranes for gas separation, Korean J. Chem. Eng. 18 (2001) 106–112.
[44] S. Giessler, L. Jordan, J.C. Diniz da Costa, G.Q. (Max) Lu, Performance of hydrophobic and hydrophilic silica membrane reactors for the water gas shift reaction, Sep. Purif. Technol. 32 (2003) 255–264.
[45] G.R. Gallaher, P.K.T. Liu, Characterization of ceramic membranes I. Thermal and hydrothermal stabilities of commercial 40 Å membranes, J. Membr. Sci. 92 (1994) 29–44.
[46] R. Leboda, E. Mendyka, A. Gieraka, V.A. Tertykh, Hydrothermal modification of silica gels (xerogels) 1. Effect of treatment temperature on their porous structure, Colloids Surf. A 105 (1995) 181–189.
[47] Q. Wei, J.-L. Li, C.-L. Song, W. Liu, C.-S. Chen, Preparation, characterization and hydrothermal stability of hydrophobic methyl-modified silica membranes, J. Inorg. Mater. 19 (2004) 417–423.